Single and double K-shell ionization and electron-transfer cross sections for Fe and Ni bombarded by S ions and Fe by Si ions at 1.25–4.70 MeV/amu

L. C. Tribedi, K. G. Prasad, and P. N. Tandon
Tata Institute of Fundamental Research, Bombay 400 005, India

Z. Chen and C. D. Lin
Department of Physics, Kansas State University, Manhattan, Kansas 66506

(Received 3 September 1993)

Single and double K-shell-vacancy production and K-K electron-transfer cross sections have been measured in the limit of zero target thickness for Fe and Ni induced by 1.25–4.70 MeV/amu ^{28}Si and ^{32}S ions. The fluorescence yield ω_K for Fe and Ni at x-ray emission was determined from the measured energy shifts of target K x rays, the intensity ratios of $K\beta$ and $K\alpha$ and using the statistical scaling procedure of Larkins [J. Phys. B **4**, L29 (1971)]. The single-electron-transfer cross sections are compared with the atomic-orbital-expansion model (AO) of Fritsch and Lin [Phys. Rep. **202**, 1 (1991)], and the semiempirical perturbed-stationary-state (PSS) approach of Lapicki and McDaniel [Phys. Rev. A **22**, 1896 (1980)]. The AO calculations show excellent agreement with the single K-K transfer cross sections. This model also explains the double K-K transfer data quite well although it underestimates slightly the measured values. The direct K-shell ionization cross section data are compared with the ECPSSR (perturbed-stationary-state theory with energy-loss, Coulomb deflection, and relativistic corrections) calculations.

PACS number(s): 34.50.Fa, 34.70.+e

I. INTRODUCTION

The K-K electron transfer is known to be an important mechanism for target K-shell vacancy production in nearly symmetric ion-atom collisions involving fully stripped and H-like heavy ions as projectiles. Its dominance over the direct K-shell ionization has been investigated in detail [1] for asymmetric and nearly symmetric collision systems using Ti as the target and various heavy ion beams up to Cl as the projectiles in the low- and intermediate-energy ranges. The two-state atomic-expansion (TSAE) model, developed by Lin and co-workers [2,3] based on the formulation given by Bates [4], is found to be very successful to explain these data on the K-K transfer cross section for nearly symmetric collision systems. However, the same model was found to overestimate the measured data for asymmetric systems (see for example the data on F $\rightarrow$ Ti and F $\rightarrow$Si in Refs. [1] and [5], respectively). These calculations have been extended by Fritsch and Lin [6] to include more numbers of atomic orbitals (AO's) of both target and projectile (instead of two states as in TSAE) in the atomic-wavefunction expansion model. The single and double K-K electron-transfer cross sections, measured recently [7] for Si and S ions bombarding the Ti target, were found to be in good agreement with these AO calculations [6]. In order to test the prediction of AO calculations for asymmetric collision systems we have measured the single and double K-K transfer cross sections for the collision system Si or S$\rightarrow$Fe and S$\rightarrow$Ni (Z_1/Z_2= 0.54–0.62, where subscripts 1 and 2 refer to projectile and target, respectively). We report here the K-K transfer as well as the direct K-shell ionization cross sections for Fe and Ni bombarded by these ions at energies varying between 1.25 and 4.70 MeV/amu. This energy region corresponds to low- to intermediate-energy range (v_1/v_{2K}= 0.28–0.60) where the K-shell ionization cross sections are sensitive to the increased binding-energy and Coulomb-deflection effects and are influenced by the sharing of the vacancies among various transient molecular orbitals. The K-K transfer cross section data are also compared with the semiempirical perturbed stationary-state formulation developed by Lapicki and co-workers [8], by including the effects due to the Coulomb deflection and increased binding energy in the Oppenheimer-Brinkman-Kramers-Nikolaev (OBKN) approximation [9].

The K-shell ionization cross sections obtained in the measurements are compared with the Coulomb ionization theory (ECPSSR) based on the perturbed stationary state (PSS) approach in which the effects due to the energy (E) loss of the projectile during the collision, Coulomb (C) deflection of the projectile in the field of the target nucleus, and relativistic (R) electron motion are incorporated in the plane-wave Born approximation [10].

II. EXPERIMENTAL DETAILS

The experimental details and the measurement techniques are described in our earlier papers [7,11] and hence only a brief outline will be provided. Si and S beams of energy varying between 1.5 and 4.7 MeV/amu were obtained from the BARC-TIFR Pelletron accelerator at Bombay. The mass and energy analyzed beam was passed through a carbon-foil stripper [12] to produce ions of different charge states. The ion beams of

required charge states, selected using a switching magnet, were made to fall on thin carbon-backed targets of Fe and Ni of various thicknesses mounted on a multiple target holder [13] in an electrically isolated chamber. The emerging beam was scattered at 120° from a gold foil of known thickness kept 6 cm downstream and provided an independent normalization of the beam current, apart from the charge collected from the beam dump and the chamber. The x rays emitted from the target were detected in two Si(Li) detectors of known efficiency [14] (with a 25-μm Be window and 170-eV resolution at 5.9 keV) mounted face to face outside the chamber at 90° to the beam direction. Each detector was separated from the chamber with the help of another Be window of 25-μm thickness holding vacuum ($\sim 5 \times 10^{-7}$ torr) inside the chamber. The total count rate in each detector was kept below 600 counts/s by using suitable absorbers of accurately known thicknesses to reduce the projectile x rays. The thicknesses of the targets were obtained during the measurement by counting the Rutherford scattered particles, at 60° with respect to the beam direction, at the lowest energy of the beams used. All the four spectra, two x-ray and two particle, were recorded simultaneously on a PC based data acquisition system.

III. DATA ANALYSIS AND RESULTS

A typical x-ray spectrum obtained using fully stripped Si ions at 125 MeV beam energy is shown in Fig. 1. The intensities of the $K\alpha$ and $K\beta$ components, due to the decay of a single K-vacancy state, as well as the hypersatellite component $K\alpha^h$, due to the decay of double K-vacancy state, were obtained from a fit to the composite spectrum using Gaussian peak shapes and a linear background. The $K\alpha$ hypersatellite intensity was used to study the double K-vacancy production cross sections [1,7]. The measured intensities were corrected for the absorber thickness, and the normalized yields were used for further data analysis. It is known that the heavy ion induced x-ray production cross section in a solid target is dependent on its thickness [15]. This is seen from Fig. 2 which shows three sets of data exhibiting the thickness dependence of the total K x-ray production cross section for Ni [Fig. 2(a)] and Fe [Figs. 2(b) and 2(c)] induced by S and Si beams with different charge states having i (i= 0, 1, or 2) K-shell vacancies. All the data with different charge states and having the same energy were fitted simultaneously, using a three-component model [16,17], to the following equation:

$$\sigma_{KX}^{i} = \frac{\sigma_{K0}}{x} \int_0^x [1 + (\alpha - 1)F_1^i(x) + (\beta - 1)F_2^i(x)]\, dx \ , \tag{1}$$

where $F_1^i(x)$ and $F_2^i(x)$ are probabilities for the projectile to have a single or double K-shell vacancy, respectively, after traversing a thickness x of the target. These probabilities are dependent on the projectile cross sections σ_{jf} (j, f=0,1,2) which are functions of Z_1, Z_2, and E_1 [15,16] and represent the cross sections for the transition from a state with j K-vacancies to a state with f

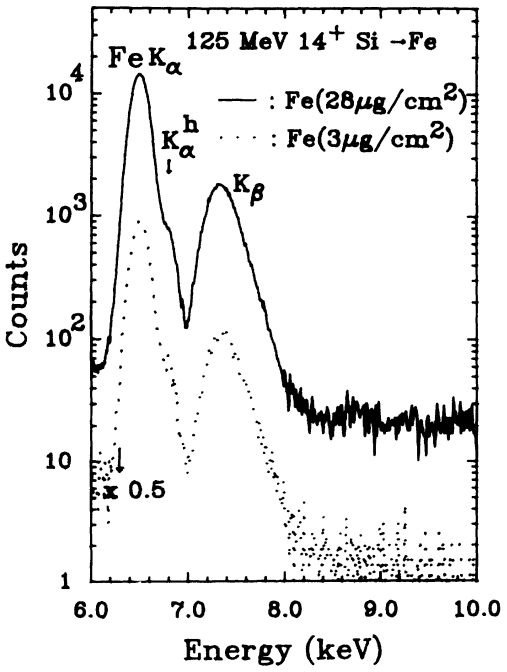

FIG. 1. A typical spectrum showing the $K\alpha$, K_α^h, K_β, x rays of Fe obtained by the bombardment of a fully stripped 125-MeV Si beam.

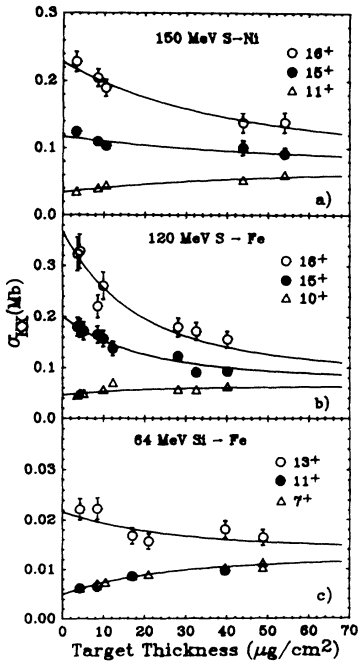

FIG. 2. Thickness dependence of average target K x-ray production cross sections for Fe and Ni bombarded by Si or S beams at different energies, as mentioned in the figure. The data for different charge states of the ions, at a given energy, were fitted simultaneously to the three-component model (solid lines). See text for details.

K-vacancies . The quantities α and β are given by the following relations:

$$\alpha = \sigma_{K1}/\sigma_{K0}\,, \quad \beta = \sigma_{K2}/\sigma_{K0}\,, \tag{2}$$

where σ_{K0}, σ_{K1}, and σ_{K2} are the zero thickness values of target K x-ray production cross sections for incident projectiles having 0, 1, or 2 K vacancies, respectively. The continuous lines in Fig. 2 denote simultaneous fits to the data of all the charge states at a given energy to Eq. (1) (for details see Refs. [7,11,17]). These fits provided the cross sections for target K x-ray production, σ^i_{KX}, in the limit of zero target thickness and are used for further analysis. At lower bombarding energies, where fully stripped beams could not be obtained, the data were fitted to the two-component model [11]. Assuming the fluorescence yield ω_K for single and double K-vacancy states to be similar [1], the corresponding vacancy production cross sections, σ^i_{SKV} and σ^i_{DKV}, are then derived from the total K-shell ionization cross section, σ^i_{KI}, using the relation

$$\sigma^i_{DKV} = \sigma^i_{KI}\frac{N^h_\alpha}{N_\alpha(\mathrm{tot})} \tag{3}$$

where $N^h_\alpha/N_\alpha(\mathrm{tot})$ is the fraction of the hypersatellite component in the total $K\alpha$ x ray. The SKV cross sections, corrected for the cascade from the decay of double vacancy, are given by

$$\sigma^i_{\mathrm{SKV}} = \sigma^i_{KI} - 2\sigma^i_{\mathrm{DKV}}\,. \tag{4}$$

As in our earlier work [7], the value of ω_K was derived from the measured values of the energy shifts of the $K\alpha$ and $K\beta$ components and their intensity ratios. Correlating these shifts and ratios with the average number of $2p$ and $3p$ vacancies and using the statistical scaling procedure of Larkins [18] the ω_K values were obtained at all the energies of Si and S ions. These values were found to be constant to within 3% over the entire energy range of the incident beam. An average value of ω_K=0.43(2) and 0.50(2) was used for Fe and Ni, respectively, for calculating the ionization cross sections. Figures 3 and 4 (see also Table I) show the σ^0_{SKV} values, i.e., direct Coulomb ionization cross sections for various beam energies used. The dashed lines shown in Figs. 3 and 4 represent the ECPSSR calculations for the systems investigated (for details see the figure caption). It can be seen that these calculations do not account for all the measured cross sections. This is more obvious from Fig. 5 in which the reduced cross sections for direct Coulomb ionization are plotted against the dimensionless quantity $\eta_K/(\zeta_K\theta_K)^2$, where η_K is the reduced energy variable and θ_K the reduced K-shell binding energy [10]. The correction due to the increased binding (B) energy or polarization (P) effects, in the plane-wave Born approximation (PWBA) for calculating the direct Coulomb ionization cross section, is expressed by the quantity ζ_K. The details of this formalism, known as PWBABCP, can be found in Refs. [10,19]. The figure shows, in a universal representation, all our data on Ti [7] and present data on Fe and Ni targets as well as of Hall *et al.* [1] for Ti targets bombarded by S ions. This figure also includes the data of Tanis *et al.* [20] for K, Ti, and Br targets bombarded by Cl ions. The ECPSSR calculations, which give a very good agreement with the proton and helium projectiles [19], show large deviations for the heavier ions used in the present case. Below a value of 0.15 for the quantity $\eta_K/(\zeta_K\theta_K)^2$, the theory underestimates the data, while above this it overestimates the data. It can also be seen that all the data do not fall on a smooth universal curve, which is very obvious for the near-symmetric collision systems in the low-energy region. For example, the cross sections for Cl on K [20] (Z_1/Z_2=0.9) show the largest deviation from the ECPSSR theory, whereas the data for asymmetric systems like Si on Fe and Cl on Br [20] (Z_1/Z_2=0.54, 0.48, respectively) show smaller deviations. The inset to Fig. 5 shows the ratio (R) of the measured cross section data, obtained in the present work, to the calculated ECPSSR values, thus representing the deviations from the theory. The large deviation of the ECPSSR theory for the near-symmetric systems clearly indicates that this semiempirical approach based on the pertur-

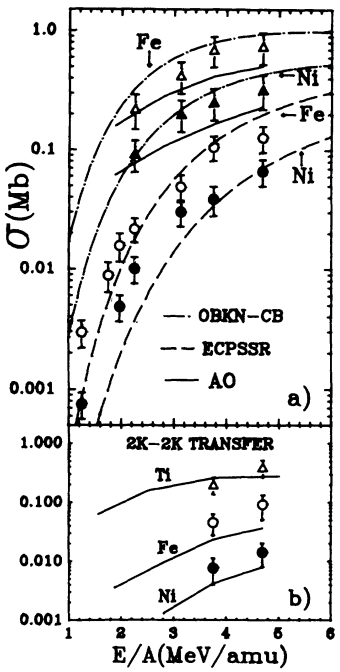

FIG. 3. (a) The direct Coulomb ionization (σ^0_{SKV}), single and double K-K transfer ($\sigma^{K\text{-}K}_{\mathrm{SKV}}$ and $\sigma^{2K\text{-}2K}_{\mathrm{DKV}}$) cross sections for Ni and Fe targets bombarded by S ions as a function of beam energy. The open and filled circles correspond to σ^0_{SKV} values for Fe and Ni, respectively. The upper (lower) dashed line represents the ECPSSR calculations [10] for S on Fe(Ni). The cross sections $\sigma^{K\text{-}K}_{\mathrm{SKV}}$ for Fe and Ni are shown by open and filled triangles, respectively. The upper (lower) solid line represents the AO model calculations [6] of K-K transfer cross sections for S on Fe (Ni). The upper (lower) dashed-dotted lines show the OBKN-CB calculations for K-K-electron transfer in case of S on Fe (Ni) in the semiempirical PSS approach [8]. (b) The double K-K transfer cross sections for S on Ti [7] (open triangle), Fe (open circle), and Ni (filled circle). The solid lines correspond to the AO calculations for three different targets as indicated.

bation method cannot describe impact ionization cross sections for near symmetric systems.

The single K-K electron-transfer cross sections from the target to the projectile are deduced from the σ^i_{KX} values using the following relation [1,7]:

$$\sigma^{K\text{-}K}_{\rm SKV} = \sigma^2_{\rm SKV} - \sigma^0_{\rm SKV} = \frac{(\sigma^1_{\rm SKV} - \sigma^0_{\rm SKV})}{\kappa} \ . \qquad (5)$$

A value of κ=0.5 was used [1,7] for deriving the values for $\sigma^{K\text{-}K}_{\rm SKV}$ at beam energies where fully stripped ions were not used (see Refs. [1,7]). The deduced values for $\sigma^{K\text{-}K}_{\rm SKV}$ (average error $\sim$ 25%) are shown in Figs. 3(a) and 4 (also see Table I) for different collision systems. The predictions of various theoretical models are also shown. The calculations based on the semiempirical formalism of Lapicki and McDaniel [8], in the PSS approach (dashed-dotted lines), including the second Born term and effects of increased binding energy and Coulomb deflection in the Oppenheimer-Brinkman-Kramers-Nikolaev approximation (OBKN-CB), explain the present set of data qualitatively quite well. For Si on Fe, this model overestimates the data by about 20–40 % but for S on Fe and Ni it provides a very good agreement. It has been shown previously [7] that this model overestimates the K-K transfer data by a factor of 2 in the case of near-symmetric collision systems like S or Si→ Ti. These observations are consistent with the fact that the perturbative approach is applicable for more asymmetric collision systems. It will be interesting to see whether these calculations provide a better agreement with the data of other heavy and asymmetric collision systems.

TABLE I. The single and double $K-K$ transfer cross sections of Fe and Ni along with the direct Coulomb ionization cross sections. All cross sections are in units of Mb. The typical errors in $\sigma^0_{\rm SKV}$, $\sigma^{K-K}_{\rm SKV}$ and $\sigma^{2K-2K}_{\rm DKV}$ are about 25%, 30%, and 35–45 %, respectively.

Beam	Target	E (MeV)/amu	$\sigma^0_{\rm SKV}$	$\sigma^{K\text{-}K}_{\rm SKV}$	$\sigma^{2K\text{-}2K}_{\rm SKV}$
Si	Fe	1.39	2.8×10^{-3}		
		1.75	4.4×10^{-3}	0.037	
		2.29	0.012	0.082	
		3.00	0.031	0.145	2.79×10^{-3}
		4.46	0.072	0.276	0.014
S	Fe	1.25	2.93×10^{-3}		
		1.75	8.79×10^{-3}		
		1.97	0.0156		
		2.25	0.0215	0.22	
		3.13	0.049	0.42	
		3.75	0.105	0.69	0.045
		4.69	0.126	0.74	0.091
S	Ni	1.25	7.5×10^{-4}		
		1.97	4.8×10^{-3}		
		2.25	0.010	0.092	
		3.13	0.030	0.20	
		3.75	0.038	0.251	7.6×10^{-3}
		4.69	0.066	0.321	0.014

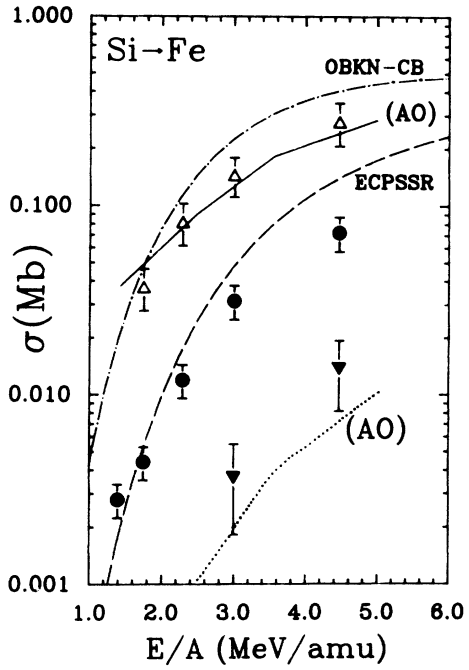

FIG. 4. The direct Coulomb ionization ($\sigma^0_{\rm SKV}$), single and double K-K transfer ($\sigma^{K\text{-}K}_{\rm SKV}$ and $\sigma^{2K\text{-}2K}_{\rm DKV}$) cross sections for Fe bombarded by Si ions as a function of beam energy. The filled circles correspond to $\sigma^0_{\rm SKV}$ values and the dashed lines represent the corresponding ECPSSR calculations [10]. The K-K transfer cross sections are denoted by the open triangles and the solid lines passing through these points represent the close-coupling AO calculations [6]. The dashed-dotted line shows the OBKN-CB calculations for K-K electron transfer given by Lapicki and McDaniel [8]. The filled inverse triangles represent the double K-K transfer cross sections for Si on Fe and the dotted line correspond to the AO calculations for these cross sections.

It can be seen from Figs. 3(a) and 4 that the atomic orbital calculations [6] (solid lines) show an excellent agreement with the K-K transfer cross section data in the energy range investigated here. Similar calculations were also shown to give a good quantitative agreement with the measured cross sections for more symmetric systems like Si and S on Ti [1,7]. However, discrepancies were found between TSAE calculations and the K-K transfer cross section data for asymmetric systems like F→Si and Ti (see Refs. [1,5]). In the present measurements the data for the asymmetric system like Si-Fe ($Z_1/Z_2 = 0.54$) show an excellent agreement (Fig. 4) with the AO calculations.

The double-K-vacancy (DKV) production cross sections [see Eq. (3)] were significant for fully stripped ions with energy more than 3 MeV/amu. These cross sections for Fe and Ni targets were deduced from the analysis of the $K\alpha$ hypersatellite using the Gaussian peak fitting procedure. The charge-state dependence of the DKV cross sections can be expressed as [1]:

$$\sigma^0_{\rm DKV} = \sigma^{K,K\text{-}L}_{\rm DKV}(q \le Z_1 - 2) \ ,$$

$$\sigma^1_{\rm DKV} = \sigma^0_{\rm DKV} + \kappa\sigma^{K\text{-}L;K\text{-}K}_{\rm DKV}(q = Z_1 - 1) \ ,$$

$$\sigma^2_{\rm DKV} = \sigma^0_{\rm DKV} + \sigma^{K\text{-}L;K\text{-}K}_{\rm DKV} + \sigma^{2K\text{-}2K}_{DKV}(q = Z_1) \ .$$

The measured charge-state dependence of DKV cross sections for Si on Fe are shown in Fig. 6(a) at two different beam energies. For ions having a filled K shell,

the DKV cross section ($\sigma^0_{\rm DKV}$) is negligibly small and is mainly contributed to by double K-shell ionization and double K-electron transfer to outer shells like L, M, etc., of the projectile. This ($\sigma^{K,K\text{-}L}_{\rm DKV}$) also includes the DKV production by K ionization simultaneously with K-shell electron transfer to outer shells. The quantity $\sigma^{K\text{-}L;K\text{-}K}_{\rm DKV}$ corresponds to the contribution due to direct ionization, excitation, or K-L, K-M, or K-N... electron transfer simultaneous with K-K transfer. The addition of this term results in the enhancement of DKV cross sections for H-like ions over $\sigma^0_{\rm DKV}$, as can be seen from Fig. 6. The dramatic increase of the DKV cross section for fully stripped ions is understood as a result of the onset of double $K-K$ electron-transfer ($2K$-$2K$ transfer) process and is expressed by the cross section $\sigma^{2K\text{-}2K}_{\rm DKV}$ which can be derived from the above equations and is given by (using $\kappa = 0.5$ [1,7])

$$\sigma^{2K\text{-}2K}_{\rm DKV} = \sigma^2_{\rm DKV} - 2\sigma^1_{\rm DKV} + \sigma^0_{\rm DKV}. \qquad (6)$$

It is also obvious from Fig. 6(a) that DKV cross sections increase with the increase in beam energy. The double K-K electron-transfer cross sections, $\sigma^{2K\text{-}2K}_{\rm DKV}$, [us-

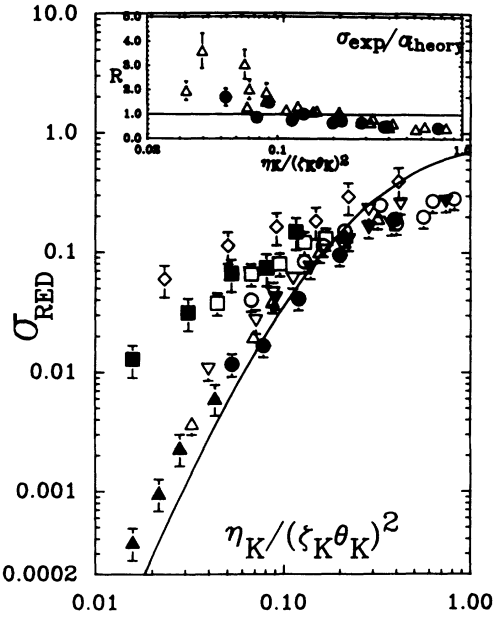

FIG. 5. The reduced cross section ($\sigma_{\rm RED}$) for direct Coulomb ionization including the effects of increased binding energy, Coulomb deflection, and polarization corrections plotted against the scaled parameter $\eta_K/(\zeta_K\theta_K)^2$. The data for S on Ti, Fe, and Ni are denoted by open circles, triangles, and inverted triangles, respectively, and those for Si on Ti and Fe are by filled inverted triangles and filled circles, respectively. The data for S and Si on Ti are taken from our earlier work [7] and those for S on Ti taken from Ref. [1] are shown by open squares. The data of Tanis *et al.* [20] for Cl on K, Ti, and Br are shown by open diamonds, filled squares, and triangles, respectively. The solid line represents the universal PWBA function [10,19]. The inset shows the ratio R=$\sigma_{\rm exp}/\sigma_{\rm theory}$ for the present collision systems to bring out the deviations in the measured cross sections from the theory. The filled circles and open triangles represent the data for Si and S beams, respectively.

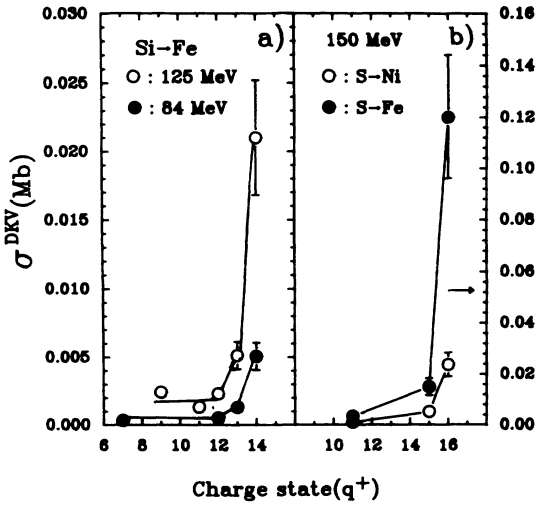

FIG. 6. The charge-state dependence of double K-shell vacancy production cross sections ($\sigma^i_{\rm DKV}$) for, (a) 125 and 84 MeV Si ions on Fe and (b) 150 MeV S ions on Fe and Ni. The dramatic increase in this cross section with fully stripped beams is obvious in both cases. The lines drawn are to guide the eye.

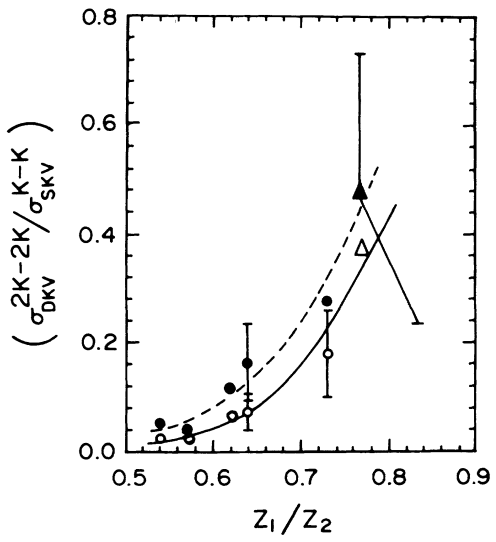

FIG. 7. The ratio of the double ($\sigma^{2K\text{-}2K}_{\rm DKV}$) to single K-K transfer ($\sigma^{K\text{-}K}_{\rm SKV}$) cross sections, for fully stripped Si, S, and Cl ions, as a function of the symmetry parameter Z_1/Z_2 for Z_2=22, 26, and 28, investigated in the present and in earlier study. The data for Cl on Ti ($Z_1/Z_2 = 0.77$), shown as open and filled triangles, are taken from Ref. [1]. All the available data for S (at 3.75 MeV/amu), Si (at 3 MeV/amu), and Cl (at 3 MeV/amu) are grouped together (open symbols) and joined through a solid line. Similarly, the closed symbols represent the data for Si 4.46 MeV/amu, S 4.69 MeV/amu, and Cl 4.5 MeV/amu ions. The closed triangle which represents the data at 4.5 MeV/amu is obtained by interpolating the data at 4 and 5 MeV/amu for which the ratios are almost constant ($\sim$ 48%) [1].

ing Eq. (6)] are shown in Figs. 3(b) and 4 (filled inverse triangles) for different collision systems (average errors 35–45 %). The AO calculations for *2K-2K* transfer are also shown. The energy dependence of these data are qualitatively explained by the AO model, though it systematically underestimates it by about 40–50% for all the three systems. Considering the fact that the measured data have relatively larger errors (~35–45 %) the deviations are not very significant. Such deviations in the double *K-K* transfer data were not observed in case of relatively symmetric systems like S or Si on Ti [1,7]. The data and calculations for S on Ti (taken from [7]) are included in Fig. 3(b) for completeness.

In Fig. 6(b) a comparison of the DKV cross sections for Fe and Ni is presented as a function of the charge state of S ions of energy 4.7 MeV/amu. The DKV cross sections for H-like or bare ions show a large increase in case of Fe over that for Ni and reflect the strong dependence of the *2K-2K* transfer cross sections on the matching of initial- and final-state binding-energies. This is more obvious from Fig. 7 in which the ratio of the double ($\sigma_{\rm DKV}^{2K\text{-}2K}$) to single *K-K* transfer ($\sigma_{\rm SKV}^{K\text{-}K}$) cross sections, for fully stripped ions, are plotted as a function of the symmetry parameter Z_1/Z_2. It is seen that R increases sharply from 4.4% to 48% for Z_1/Z_2 changing from 0.57 (S on Ni at 4.7 MeV/amu) to 0.77 (Cl on Ti at 4.5 MeV/amu [1]). The solid (dashed) line joining the open (filled) points are used to guide the eye (see figure caption for details). The increase of this ratio with increasing Z_1/Z_2 can be qualitatively understood in the following way. It is known that the probability of single electron transfer, $P(b)$ at impact parameter b, increases sharply as the ratio Z_1/Z_2 approaches unity due to favorable matching of binding energies. Since the leading term in $\sigma_{\rm SKV}^{K\text{-}K}$ goes as $\sim P$ and $\sigma_{\rm DKV}^{2K\text{-}2K}$ goes as $\sim P^2$, the ratio R is proportional to $\sim P$ which increases with the increase of Z_1/Z_2.

IV. CONCLUSIONS

Single and double *K-K* electron-transfer and the *K*-shell vacancy production cross sections have been measured for Fe and Ni targets bombarded by S ions and Fe bombarded by Si ions in the energy range 1.25–4.70 MeV/amu. The ECPSSR theory explains the direct ionization cross section data only qualitatively for asymmetric collisions, although deviations are found at lower as well as higher energies [Figs. 3(a) and 4]. However, scaled cross sections (Fig. 5), including various corrections, for the near symmetric collision systems show larger deviations from the universal PWBA function. The calculations of Lapicki and McDaniel [8], based on a perturbative approach including the semiempirical correction factors, explain the capture cross section data quite well. An excellent agreement is found between the close-coupling AO calculations [6] and the single *K-K* electron-transfer data. These calculations also explain the double *K-K* transfer cross sections for the present asymmetric collision systems, although they underestimate the data slightly.

ACKNOWLEDGMENTS

The authors thank Dr. M. R. Press for his help in performing the Hartree-Fock calculations. They also thank the pelletron accelerator staff for the smooth running of the machine.

[1] J. Hall, P. Richard, T.J. Gray, N. Newcomb, P. Pepmiller, C. Dolmi, K. Jones, B. Johnson, and D. Gregory, Phys. Rev. A **28**, 99 (1983); J. Hall, P. Richard, P.L. Pepmiller, D.C. Gregory, P.D. Miller, C.D. Moak, C.M. Jones, G.D. Alton, L.B. Bridwell, and C.J. Sofield, *ibid.* **33**, 914 (1986).

[2] C.D. Lin, S.C. Soong, and L.N. Tunnell, Phys. Rev. A **17**, 1646 (1978); C.D. Lin and L.N. Tunnell, *ibid.* **22**, 76 (1980).

[3] C.D. Lin and P. Richard, in *Advances in Atomic and Molecular Physics*, edited by D. Bates and B. Bederson (Academic, New York, 1981), Vol. 17, p. 275, and references therein.

[4] D.R. Bates, Proc. R. Soc. London Ser. A **247**, 294 (1958).

[5] H. Tawara, P. Richard, T.J. Gray, J. Newcomb, K.A. Jamison, C. Schmiedekamp, and J.H. Hall, Phys. Rev. A **18**, 1373 (1978).

[6] W. Fritsch and C.D. Lin, Phys. Rep. **202**, 1 (1991), and references therein.

[7] L.C. Tribedi, K.G. Prasad, and P.N. Tandon, Phys. Rev. A **47**, 3739 (1993).

[8] G. Lapicki and F.D. McDaniel, Phys. Rev. A **22**, 1896 (1980); G. Lapicki and W. Losonsky, *ibid.* **15**, 896 (1977).

[9] M.R.C. McDowell and J.P. Coleman, *Introduction to the Theory of Ion-atom Collision* (North-Holland, New York, 1970), Chap. 8; V.S. Nikolaev, Zh. Eksp. Teor. Fiz. **51**, 1263 (1966) [Sov. Phys. JETP **24**, 847 (1967)].

[10] W. Brandt and J. Lapicki, Phys. Rev. A **23**, 171 (1981); G. Basbas, W. Brandt and R. Laubert, *ibid.* **17**, 1655 (1978).

[11] L.C. Tribedi, K.G. Prasad, and P.N. Tandon, Z. Phys. D **24**, 215 (1992).

[12] S.D. Narvekar, R.R. Hosangdi, L.C. Tribedi, R.G. Pillay, K.G. Prasad, and P.N. Tandon, Pramana J. Phys. **39**, 79 (1992).

[13] L.C. Tribedi, S.D. Narvekar, R.G. Pillay, and P.N. Tandon, Pramana J. Phys. **46**, 661 (1992).

[14] L.C. Tribedi and P.N. Tandon, Nucl. Instrum. Methods B **62**, 178 (1992).

[15] See, e.g., T.J. Gray, in *Methods of Experimental Physics*, edited by P. Richard (Academic Press, New York, 1980), Vol. 17, p. 193.

[16] S.K. Allison, Rev. Mod. Phys. **30**, 1137 (1958).

[17] R.K. Gardner, T.J. Gray, P. Richard, C. Schmiedekamp, K.A. Jannison, and J.M. Hall, Phys. Rev. A **15**, 2202 (1977).

[18] F.P. Larkins, J. Phys. B **4**, L29 (1971).

[19] L.C. Tribedi and P.N. Tandon, Phys. Rev. A **45**, 7860 (1992); **46**, 4425 (1992).

[20] J.A. Tanis, S.M. Shafroth, W.W. Jacobs, T. McAbee, and G. Lapicki, Phys. Rev. A **31**, 750 (1985).